



ELSEVIER

Available online at www.sciencedirect.com

SCIENCE @ DIRECT®

Materials Letters 57 (2003) 3048–3056

**MATERIALS
LETTERS**

www.elsevier.com/locate/matlet

Mechanical properties and oxidation resistance of $\text{Ti}_3\text{SiC}_2/\text{SiC}$ composite synthesized by in situ displacement reaction of Si and TiC

Shi-Bo Li^{a,*}, Jian-Xin Xie^a, Li-Tong Zhang^b, Lai-Fei Cheng^b

^a*School of Materials Science and Engineering, University of Science and Technology Beijing, Beijing 100083, China*

^b*State Key Laboratory of Solidification Processing, Northwestern Polytechnical University, Xian, Shaanxi 710072, China*

Received 24 September 2002; received in revised form 4 December 2002; accepted 9 December 2002

Abstract

$\text{Ti}_3\text{SiC}_2/\text{SiC}$ composite has been synthesized by in situ displacement reaction of Si and TiC powders. Its relative density is >98%. Its Vickers hardness was measured to be 8.7 GPa. Its flexural strength and the fracture toughness were 505 MPa and 5.3 $\text{MPa}\cdot\text{m}^{1/2}$, respectively. Scanning electron micrograph (SEM) and transmission electron micrograph (TEM) were used to observe the microstructure of the composite. Mechanisms for its high flexural strength and fracture toughness were discussed, respectively. The composite shows a better oxidation resistance than monolithic Ti_3SiC_2 at high temperatures. The oxidation layers were comprised of an outer layer with coarse TiO_2 grains and an inner layer with a mixture of fine-grained SiO_2 and TiO_2 . Its weight gain is only about 7.9 mg/cm^2 at 1200 °C in air for 21 h. However, that of Ti_3SiC_2 is 30 mg/cm^2 . The results suggested that the in situ formation of SiC improved its oxidation resistance.

© 2002 Elsevier Science B.V. All rights reserved.

Keywords: In situ synthesis; $\text{Ti}_3\text{SiC}_2/\text{SiC}$ composite; Microstructure; Mechanical properties; Oxidation resistance

1. Introduction

Ti_3SiC_2 with layered structure is just like boron nitride (BN) or graphite. However, it is stronger in mechanical properties and better in oxidation resistance than boron nitride or graphite. Recently, this ternary compound has attracted much attention because it has high toughness (6–11 $\text{MPa}\cdot\text{m}^{1/2}$) [1–3], high Young's modulus (320 GPa) [4,5], low hardness (about 4 GPa) [6,7], and moderate flexural

strength (260–600 MPa) [2,3,8]. Furthermore, it exhibits plasticity at high temperature, good electrical conductivity, high thermal shock resistance, and easy machinability. Because of these better properties mentioned above, it is expected to apply in various fields. For example, it can be used as a structural ceramic for high-temperature application, an excellent candidate for metal smelting, in general, and a promising candidate for bearings, kiln furniture, wear and corrosion protection, etc. [4,9,10]. Recently, Gao and Miyamoto [11] also reported that Ti_3SiC_2 exhibits good biocompatibility, no biotoxicity, and high corrosion resistance in 0.9 % NaCl solution, suggesting the possibility of bioinert ceramic.

* Corresponding author. Tel.: +86-10-62333999; fax: +86-10-62334311.

E-mail address: shibo-li@sohu.com (S.-B. Li).

Ti_3SiC_2 can be strengthened by thermodynamically stable inclusions such as SiC, TiC, and silicides. For example, $\text{Ti}_3\text{SiC}_2/\text{TiC}$ or $\text{Ti}_3\text{SiC}_2/\text{SiC}$ composites exhibited better mechanical properties than monolithic Ti_3SiC_2 . Rudnik and Lis [12] reported the compressive and three-point bending strengths of Ti_3SiC_2 containing 15 vol.% TiC to be 1120 and 350 MPa, respectively. Gao et al. [3] reported that the dense bulk Ti_3SiC_2 containing 3 vol.% TiC had a flexural strength of 480 MPa and a high fracture toughness of $11.2 \text{ MPa}\cdot\text{m}^{1/2}$. Tong et al. [1] fabricated $\text{Ti}_3\text{SiC}_2/\text{SiC}$ composites that show a higher flexure strength and a lower oxidation rate than monolithic Ti_3SiC_2 .

Ti_3SiC_2 as structural application in high-temperature environment should have adequate strength, good creep resistance and oxidation resistance. Thus, Ti_3SiC_2 matrix reinforced with ceramic particles is one of the effective measures. The reinforcements should be stable in contact with Ti_3SiC_2 at high temperature and could improve the matrix properties. Thus, particle of SiC, which has good properties and good resistance to oxidation at high temperature, has been proved to be one of the promising reinforcements in many ceramics matrix. Furthermore, it is compatible and stable with Ti_3SiC_2 at high temperature [9,13].

In previous work, we have successfully synthesized SiC in situ reinforced Ti_3SiC_2 composites by displacement reaction of Si and TiC powders [14]. In this work, the main purpose is to examine the mechanical properties of $\text{Ti}_3\text{SiC}_2/\text{SiC}$ composite at room temperature. Its oxidation resistance at high temperature was compared with that of the monolithic Ti_3SiC_2 .

2. Experimental procedure

The starting powders of TiC (average particle size: $<10 \mu\text{m}$, $>99\%$ purity) and Si (average particle size: -325 mesh, $>99\%$ purity) were used to fabricate $\text{Ti}_3\text{SiC}_2/\text{SiC}$ composite. They were mixed for 10 h in a ball mixer. The mixed powders were hot-pressed at 30 MPa pressure in graphite dies coated with boron nitride (BN) under vacuum at 1350°C for 2 h to avoid Si melting, and then followed by 1500°C for 1 h for densification. The relative density of the specimen was determined by Archimedes' method. The

phase composition was identified by X-ray diffraction (XRD) and energy-dispersive X-ray analysis (EDX). The observation of fractured and polished surfaces was performed by scanning electron microscopy (SEM). Transmission electron microscope (TEM) was also used to observe the microstructure of the composite.

The specimen was cut by a diamond cutter into $3 \times 4 \times 40 \text{ mm}$ and $2 \times 4 \times 24 \text{ mm}$ bars. One face of the $3 \times 4 \times 40 \text{ mm}$ bars was polished with diamond paste and its edges were beveled for measuring the flexural strength by three-point bending test (30 mm outer span). The $2 \times 4 \times 24 \text{ mm}$ bars were machined a notch with the depth of 2 mm and the width of 0.1 mm by diamond wheel for determining the fracture toughness by single-edge notched beam (SENB) test (20 mm outer span). The Vickers indentations were made at the load range of 1–20 kg on the polished surface. The damage zones were observed by SEM. Small bars with dimension of $2 \times 4 \times 14\text{--}15 \text{ mm}$ were used for oxidation test. The oxidation test was performed in a high-temperature furnace in the temperature range of $1000\text{--}1400^\circ\text{C}$ for exposures up to 21 h. Weight gain was measured by an electric balance at interval of 3 h. After the oxidation test was finished, surfaces and cross-sections of the oxidation sample were observed and analyzed by SEM, XRD and EDX, respectively.

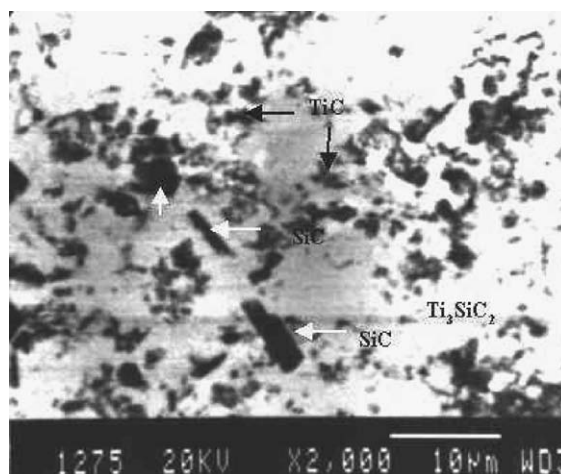


Fig. 1. Backscattered electron image taken from polished surface of $\text{Ti}_3\text{SiC}_2/\text{SiC}$ composites.

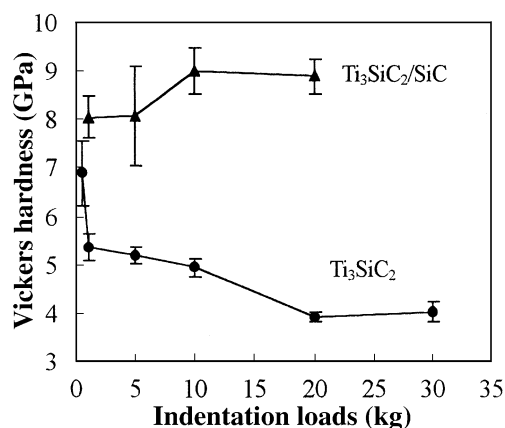


Fig. 2. Vickers hardness of $\text{Ti}_3\text{SiC}_2/\text{SiC}$ and monolithic Ti_3SiC_2 as a function of load.

3. Results and discussion

3.1. Mechanical properties at room temperature

3.1.1. Vickers hardness

Fig. 1 shows SiC particles (marked as white arrows) with platelet or blocky shape distributed in Ti_3SiC_2 matrix. The average size of blocky SiC is about $2\text{ }\mu\text{m}$. Some SiC platelets, however, are less than $6\text{ }\mu\text{m}$ in length and $2\text{ }\mu\text{m}$ in width. Particles of TiC (marked as black arrows) with about $1\text{ }\mu\text{m}$ in size were also found in this composite. The particles of SiC or TiC inhibited the grain-boundary migration of Ti_3SiC_2 resulting in a fine-grained Ti_3SiC_2 matrix with size of $10\text{ }\mu\text{m}$ [14].

Fig. 2 shows the Vickers hardness of $\text{Ti}_3\text{SiC}_2/\text{SiC}$ and Ti_3SiC_2 as a function of load. The average value of

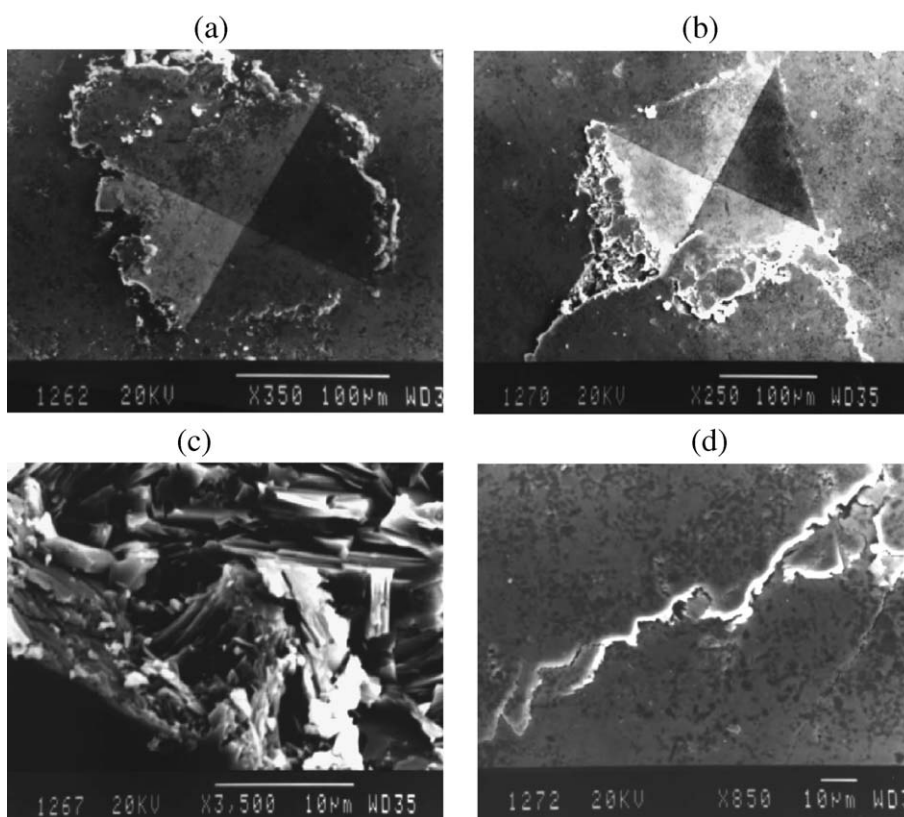


Fig. 3. Micrographs of surfaces indented with different loads. (a) 10 kg; (b) 20 kg; (c) enlarged damage zone taken from (b); and (d) crack propagation path.

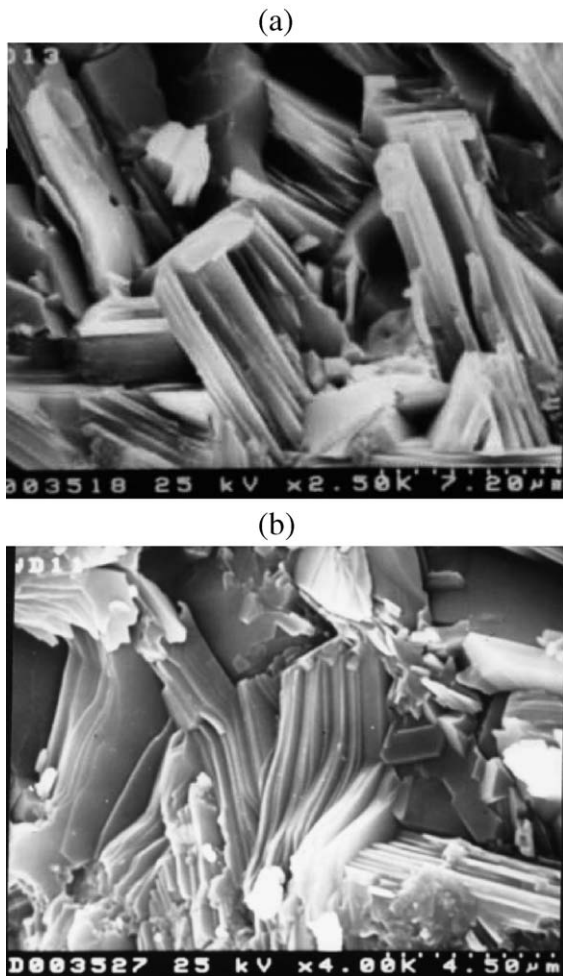


Fig. 4. Scanning electron micrographs of the fracture surface of $\text{Ti}_3\text{SiC}_2/\text{SiC}$ composite.

hardness is 8.7 GPa. The hardness value increased as the load increases from 5 to 10 kg. Then it remained unchanged. From Fig. 2, it is seen that the curve of hardness of $\text{Ti}_3\text{SiC}_2/\text{SiC}$ differed from that of monolithic Ti_3SiC_2 . The hardness of Ti_3SiC_2 decreased with increasing loads. The hardness value asymptotically approached 4 GPa as the load rose to 30 kg. The composite had a higher hardness than monolithic Ti_3SiC_2 . The main reason should be ascribed to the particles of SiC and TiC which both have high hardness.

Fig. 3(a) and (b) are Vickers indentation marks for $\text{Ti}_3\text{SiC}_2/\text{SiC}$ made by loading with 10 and 20 kg, respectively. It can be seen that broken material has been

piled up around the impression. The indentation marks exhibited asymmetric damage as shown in Fig. 3(a) that should be attributed to the anisotropy of the mechanical properties of Ti_3SiC_2 [6]. With increasing load, the damage mark became larger and larger. Indentation crack emanation from the corners can be found as the load was increased to 20 kg (Fig. 3(b)). This feature obviously differed from the observation for Ti_3SiC_2 because no cracks were found near the indentations. Around the indentations for Ti_3SiC_2 made by 30-kg load, there is a large amount of deformed grains with delamination, bending, and buckling [7] that endow Ti_3SiC_2 with damage tolerance.

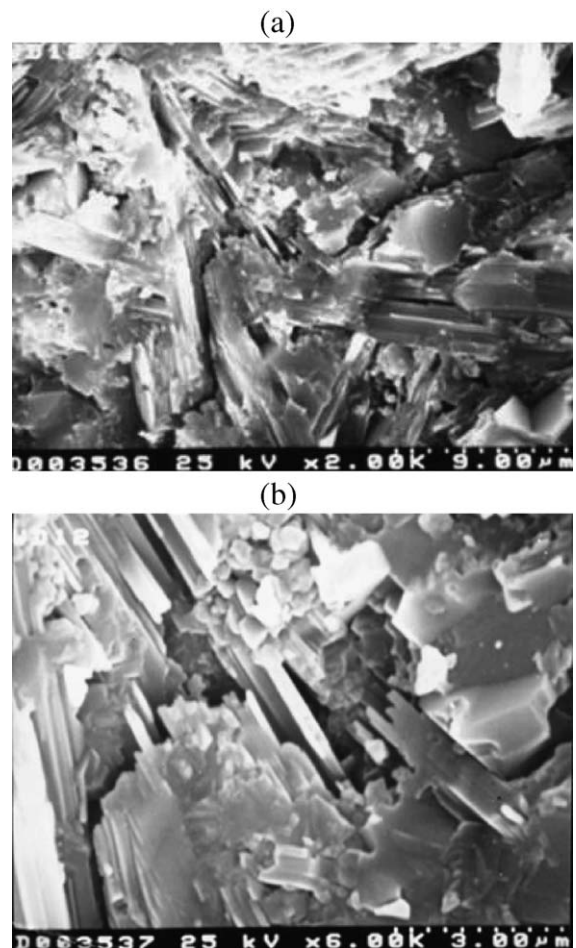


Fig. 5. Morphology of crack propagation in the fractured of $\text{Ti}_3\text{SiC}_2/\text{SiC}$ is shown in (a). (b) Higher magnification microstructure of (a).

However, for $\text{Ti}_3\text{SiC}_2/\text{SiC}$, bending and buckling grains are not found. Fig. 3(c) is the enlarged microstructure taken from the indentation of Fig. 3(b). Many grains have been broken into debris and some are delaminated. The main reason for those differences for the indentation marks between Ti_3SiC_2 and $\text{Ti}_3\text{SiC}_2/\text{SiC}$ may be resulted from the effect of grain size. The particles of SiC or TiC inhibited the grain growth of Ti_3SiC_2 and resulted in the fine-grained Ti_3SiC_2 matrix with size of $10\text{ }\mu\text{m}$ that is smaller than the monolithic Ti_3SiC_2 with size of $25\text{ }\mu\text{m}$ [15]. The larger the grain is, the easier the deformation is for

Ti_3SiC_2 . It has been proved that the coarse-grained Ti_3SiC_2 was more damage tolerant than the fine-grained [8].

Fig. 3(d) shows magnified image of crack propagation path taken from Fig. 3(b). The cracks show deflection, branching, and bridging during propagation. This feature consumed the propagation energy and benefited for improving the fracture toughness.

3.1.2. Flexural strength and fracture toughness

The fabricated composite possessed a high relative density of $>98\%$. The flexural strength and the frac-

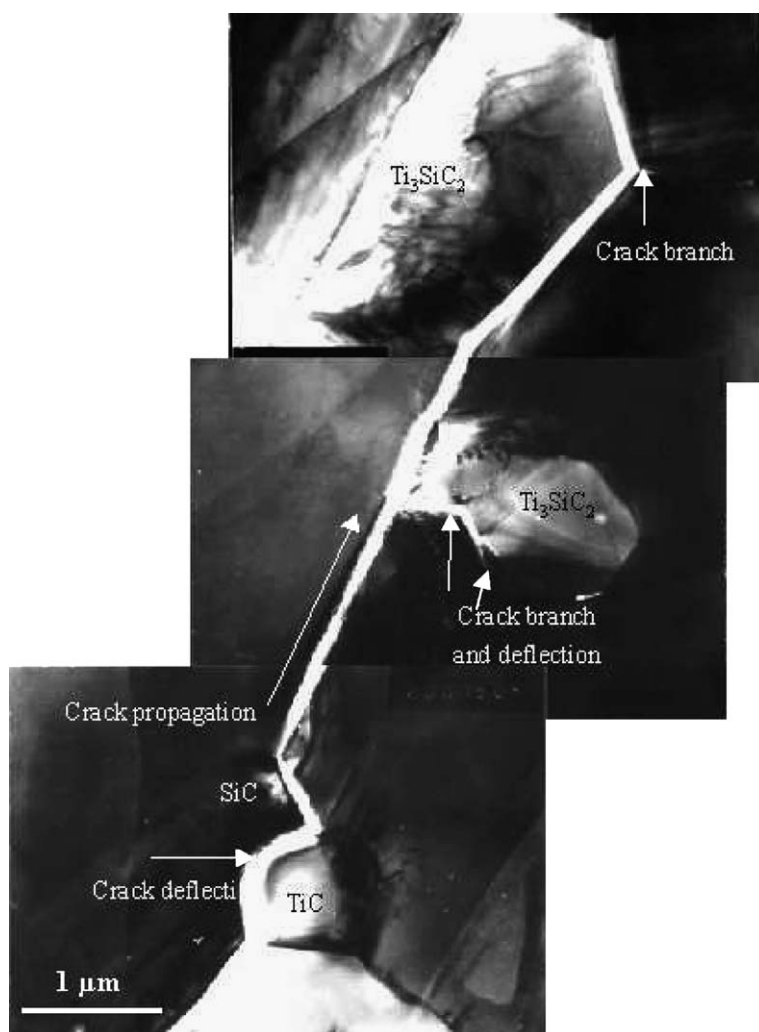


Fig. 6. TEM microstructure showing path of crack propagation.

ture toughness of SiC-reinforced Ti_3SiC_2 composite were measured to be 505 MPa and $5.3 \text{ MPa}\cdot\text{m}^{1/2}$, respectively. The monolithic Ti_3SiC_2 has a flexural strength of 300 MPa and a fracture toughness of $6 \text{ MPa}\cdot\text{m}^{1/2}$ [8]. The flexural strength of composite was higher than that of monolithic Ti_3SiC_2 ; however, the fracture toughness was lower than monolithic Ti_3SiC_2 . It indicated that the grain size had effect on the mechanical properties.

Fig. 4 shows the features of fractured surfaces of the composite. It can be seen from Fig. 4 that the fractured surfaces are rough. The elongated Ti_3SiC_2 grains with laminated character can easily be identified (Fig. 4(a)). The pull out of the elongated Ti_3SiC_2 grains can also be observed in Fig. 4(a). The surface of intragranular fractured Ti_3SiC_2 grains exhibited layered features (Fig. 4(b)). It indicated that the tensile surface was perpendicular to the basal planes of Ti_3SiC_2 and resulted in the above feature formation.

Fig. 5 shows morphology of crack propagation in the fractured surface of $\text{Ti}_3\text{SiC}_2/\text{SiC}$. The crack was deflected for more extent as it met elongated Ti_3SiC_2 grains (Fig. 5(a)). Fig. 5(b) is the higher magnification of microstructure taken from Fig. 5(a). Some Ti_3SiC_2 grains have been delaminated, but others exhibited a zigzag feature in the fractured surface (Fig. 5(b)). By combination of the features in Figs. 4 and 5, it is suggested that the grains destroyed with delamination or transgranular fracture are dependent on the direction of crack propagation. When the basal planes of Ti_3SiC_2 are parallel to direction of the crack propagation, delamination occurs by the crack propagation along the basal planes. When the basal planes are normal to the crack propagation, the crack will penetrate into grains and be deflected in the grains. Those features can consume the expansion energy of crack improving the fracture toughness of $\text{Ti}_3\text{SiC}_2/\text{SiC}$.

Fig. 6 is the TEM microstructure showing the crack propagation path. The crack propagates along the grain boundary and then is deflected as it met the particles TiC or SiC. Crack branching can also be observed in the grain boundary where the bond may be weak between two particles of Ti_3SiC_2 .

In short, the grain pull out, delamination and the crack defection, branching, and bridging are the main mechanisms for improving the fracture toughness of

$\text{Ti}_3\text{SiC}_2/\text{SiC}$ composite. The fine-grained Ti_3SiC_2 matrix and higher relative density resulted in this composite with higher flexural strength.

3.2. Oxidation behavior at high temperature

The oxidation behavior of monolithic Ti_3SiC_2 has been investigated in the temperature range of 1000–1500 °C in previous work [15]. Monolithic Ti_3SiC_2 had excellent oxidation resistance at temperature below 1100 °C.

Fig. 7 shows the weight gain of monolithic Ti_3SiC_2 and $\text{Ti}_3\text{SiC}_2/\text{SiC}$ at 1200 and 1300 °C in air. The oxidation time of $\text{Ti}_3\text{SiC}_2/\text{SiC}$ is 21 h; for monolithic Ti_3SiC_2 , it is 20 h. The oxidation resistance of $\text{Ti}_3\text{SiC}_2/\text{SiC}$ at 1200 and 1300 °C was better than that of Ti_3SiC_2 . The weight gain of $\text{Ti}_3\text{SiC}_2/\text{SiC}$ at 1200 °C for 21 h is only about $7.9 \text{ mg}/\text{cm}^2$; however, that of Ti_3SiC_2 is $30 \text{ mg}/\text{cm}^2$. For oxidation at 1300 °C for 21 h, the weight gain of the composite is $25 \text{ mg}/\text{cm}^2$ which is lower than $70 \text{ mg}/\text{cm}^2$ for Ti_3SiC_2 . The results suggested that the in situ formation of SiC improved the oxidation resistance of $\text{Ti}_3\text{SiC}_2/\text{SiC}$. Tong et al. [1] drew the same conclusion that $\text{Ti}_3\text{SiC}_2/\text{SiC}$ composite possessed better resistance to oxidation than monolithic Ti_3SiC_2 . The value of weight gain in this experiment is lower than that of Tong reported. The reason may be ascribed to the fact that in situ synthesized $\text{Ti}_3\text{SiC}_2/\text{SiC}$ has high relative density and fine-grained Ti_3SiC_2 .

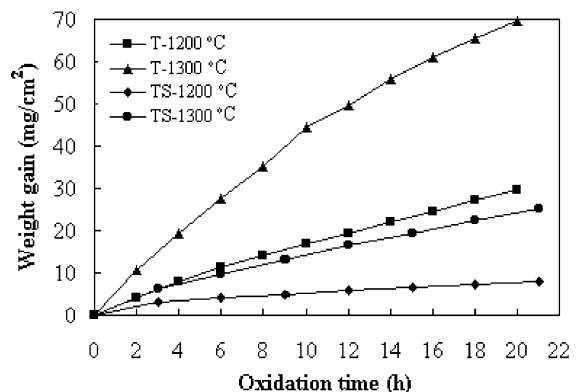


Fig. 7. Mass gain of monolithic Ti_3SiC_2 (marked “T”) and $\text{Ti}_3\text{SiC}_2/\text{SiC}$ composite (marked “TS”) as a function of oxidation time at 1200 and 1300 °C.

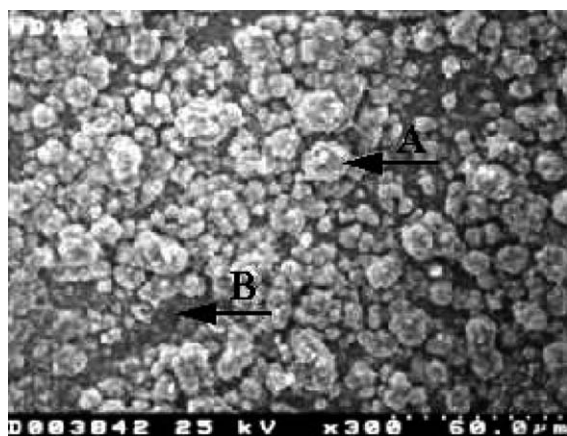


Fig. 8. SEM micrograph of oxidation surface at 1000 °C.

A SEM micrograph of oxidation surface at 1000 °C is presented in Fig. 8, showing that the oxidation surface was decorated by the white oxides that had been conglobated. Those white oxides marked “A” were TiO_2 that was identified by EDX as shown in Fig. 9(a). The areas marked “B” were identified to be a mixture of Si, O, and Ti atoms (Fig. 9(b)). It is suggested that the oxidation surface is covered with mixture of TiO_2 and SiO_2 at 1000 °C. XRD patterns also proved that both of rutile-type TiO_2 and SiO_2 presented on the surface oxidized at 1000 °C. However, the peaks of SiO_2 disappeared with increasing oxidation temperature, only leaving TiO_2 . No the presence of Si could be detected by EDX analysis,

indicating that SiO_2 did not transform to amorphous phase. This phenomenon will be discussed at the back of this section.

Fig. 10(a) and (b) shows the morphology of oxidized surfaces of $\text{Ti}_3\text{SiC}_2/\text{SiC}$ at 1200 and 1300 °C, respectively. The oxidized surfaces are covered by TiO_2 grains. There are no SiO_2 existing on the surfaces that had been identified by both XRD and EDX. It can be seen from Fig. 10(a) that TiO_2 grains are about $\sim 8 \mu\text{m}$ in size. The dense oxidation film acted as a diffusion barrier that retarded the diffusion of oxygen. That is why the composite possessed good oxidation resistance below 1200 °C. The size of TiO_2 grains increased with increasing oxidation temperature. At 1300 °C, the oxide grains grew to be $\sim 18 \mu\text{m}$. A large amount of small pores appeared on the oxidized surface as shown in Fig. 10(b). Those pores provided the channel for oxygen diffusion and accelerated the oxidation process because small pores in the scale provide short-circuit paths for oxygen transport to the oxidation interface, and quick oxidation occurs at the areas near the pores. It is consistent with the oxidation behavior of the composite at 1300 °C, the weight gain at this temperature was greater than at 1200 °C.

The pores may be resulted from Ti ions quick diffusion and escape of CO_2 . With the increasing temperature, Ti ions will diffuse through the oxidation layer to react with the oxygen at the surface and leave the cavities beneath the outer layer, this phenomenon is similar to that of metal Ni oxidation [14]. Volatili-

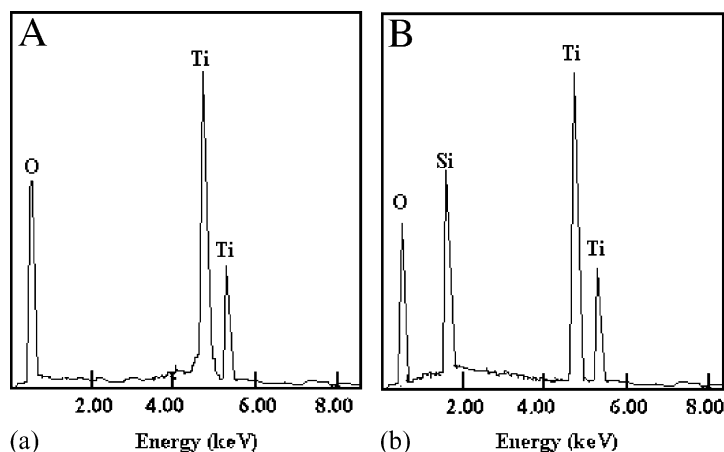


Fig. 9. EDX microanalysis of A and B areas as shown in (a) and (b) taken from Fig. 8.

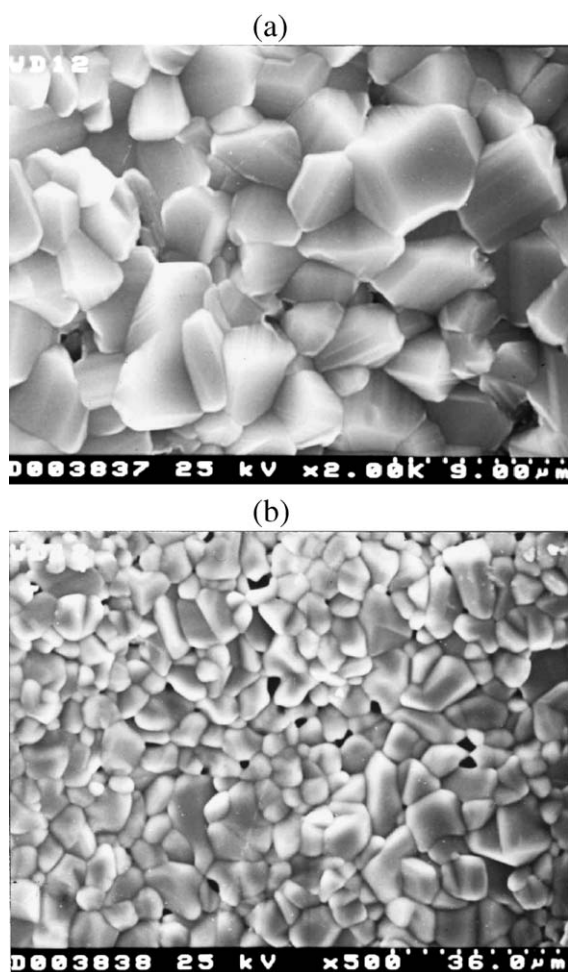
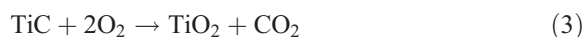
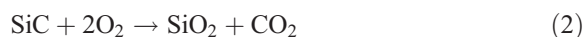
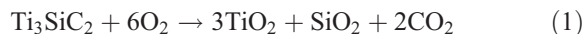


Fig. 10. Morphology of surface of $\text{Ti}_3\text{SiC}_2/\text{SiC}$ oxidized at (a) 1200 °C and (b) 1300 °C for 21 h.

zation of CO_2 can also lead to the formation of pores because three phases of Ti_3SiC_2 , SiC , and TiC all emit CO_2 as oxidized at high temperature. The equations are listed as follows:



In the case of Ti_3SiC_2 , it has a great effect on forming the pores because the composite was mainly composed of Ti_3SiC_2 . Fig. 11 shows the cross-section

of the oxidation sample at 1400 °C. Two layers formed on the oxidized surface. The outer layer was mainly composed of large TiO_2 grains, which grew to be about 40 μm in size at 1400 °C. However, the inner layer consisted of a mixture of SiO_2 and TiO_2 that were identified by EDX microanalysis. The above feature was similar to that of monolithic Ti_3SiC_2 oxidized at high temperature [15]. The mixtures of grains in the inner layer are finer than outer layers. This feature should be ascribed to the diffusion of Ti ions and the growth of TiO_2 . Barsoum and El-Raghy [16] reported that the oxidation process for Ti_3SiC_2 was controlled by the outward diffusion of Ti and C and the inward diffusion of oxygen, and Si was essentially immobile. Ti ions will diffuse fast through the SiO_2 layer and oxidize in contact with air, adding to the outer layer of TiO_2 scale. At the same time, oxygen also diffused into oxidation layers and matrix, where it met Ti and Si ions and reacted to TiO_2 and SiO_2 . After certain oxidation time, the inner layer containing a mixture of TiO_2 and SiO_2 would be formed beneath the outer layer. That is the reason why no SiO_2 could be detected by using XRD and EDX at 1200 °C. TiO_2 in the outer layer grows very quickly without any restraint and develops to the coarse grains. However, the growth of SiO_2 and TiO_2 grains in the inner layer is prevented by the outer layer and is resulted in the finer grain formation. If the oxidation layers were dense, especially for the inner layer, the oxygen diffusion would be retarded and the oxidation resistance be improved.

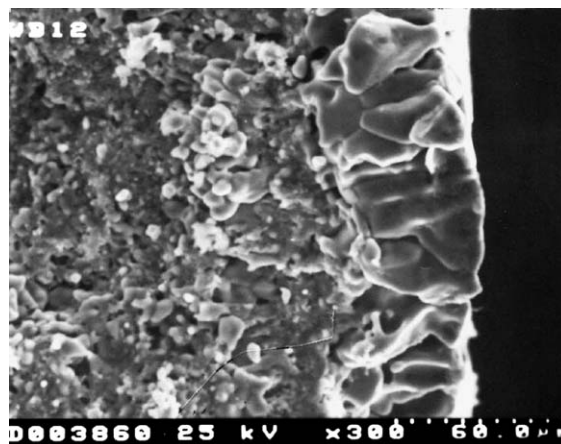


Fig. 11. Morphology of cross-section of $\text{Ti}_3\text{SiC}_2/\text{SiC}$ oxidized at 1400 °C for 21 h.

As discussed above, there are no doubts that SiC improved the oxidation resistance of $\text{Ti}_3\text{SiC}_2/\text{SiC}$. However, impurity TiC has poor oxidation resistance at high temperature ($>1000^\circ\text{C}$) because it led to the formation of TiO_2 and CO_2 . Escape of CO_2 resulted in the formation of pores in the oxide layer. Oxygen can easily penetrate through the porous layer and enhance the oxidation rate. Mitra and Rama [17] also draw the same conclusion by investigating the oxidation of $\text{Ti}_5\text{Si}_3/20$ vol.% TiC composites.

In other words, in situ formation of SiC improved the oxidation resistance of Ti_3SiC_2 . The oxidation resistance of the $\text{Ti}_3\text{SiC}_2/\text{SiC}$ composite was good below 1200°C with a weight gain of only 7.9 mg/cm^2 because of the formation of a dense oxidized film on the surface that retarded the diffusion of oxygen.

4. Conclusion

$\text{Ti}_3\text{SiC}_2/\text{SiC}$ possesses good mechanical properties and oxidation resistance. The Vickers hardness of $\text{Ti}_3\text{SiC}_2/\text{SiC}$ is about 8.7 GPa , which is larger than that of monolithic Ti_3SiC_2 . The flexural strength and the fracture toughness of SiC-reinforced Ti_3SiC_2 composite were measured to be 505 MPa and $5.3\text{ MPa}\cdot\text{m}^{1/2}$, respectively. The high relative density of the composite and the fine-grained Ti_3SiC_2 matrix are the main reasons for the high flexural strength. Grain pull out, delamination and the crack defection, branching, and bridging are the main mechanisms for improving the fracture toughness of the composite.

The composite shows a good oxidation resistance at high temperature. Its oxidation resistance at 1200 and 1300°C was better than that of Ti_3SiC_2 . Its weight gain at 1200°C is only about 7.9 mg/cm^2 . At and above 1100°C , no SiO_2 could be found again

on the oxidation surface, but it combined with TiO_2 to form the finer grains beneath the outer layer. The dense oxidized film formed on the surface acted as a diffusion barrier that retarded the diffusion of oxygen below 1300°C . The results suggested that the in situ formation of SiC improved the oxidation resistance of $\text{Ti}_3\text{SiC}_2/\text{SiC}$ composite.

References

- [1] X.H. Tong, T. Okano, T. Iseki, T. Yano, J. Mater. Sci. 30 (1995) 3087.
- [2] Y.C. Zhou, Z.M. Sun, Mater. Res. Innov. 2 (1999) 360.
- [3] N.F. Gao, Y. Miyamoto, D. Zhang, J. Mater. Sci. 34 (1999) 4385.
- [4] M.W. Barsoum, T. El-Raghy, J. Am. Ceram. Soc. 79 (1996) 1953.
- [5] R. Pampuch, J. Lis, J. Piekarczyk, L. Stobierski, J. Mater. Synth. Process. 1 (1993) 93.
- [6] T. El-Raghy, A. Zavaliangos, M.W. Barsoum, S.R. Kalidindi, J. Am. Ceram. Soc. 80 (1997) 513.
- [7] S.B. Li, L.F. Cheng, L.T. Zhang, Mater. Sci. Technol. 18 (2002) 231.
- [8] T. El-Raghy, A. Zavaliangos, M.W. Barsoum, S.R. Kalidindi, J. Am. Ceram. Soc. 82 (1999) 2860.
- [9] M.W. Barsoum, T. El-Raghy, Adv. Mater. Process. 7 (1997) 52.
- [10] M.W. Barsoum, Prog. Solid State Chem. 28 (2000) 281.
- [11] N.F. Gao, Y. Miyamoto, J. Mater. Res. 17 (2002) 59.
- [12] T. Rudnik, J. Lis, Arch. Metall. 42 (1997) 59.
- [13] B.J. Kool, M. Kabel, A.B. Kloosterman, J.Th.M. De Hosson, Acta Mater. 47 (1999) 3116.
- [14] S.B. Li, J.X. Xie, L.T. Zhang, L.F. Cheng, submitted for publication.
- [15] S.B. Li, "Microstructure and Mechanical Properties of Layered Ceramic Ti_3SiC_2 and $\text{Ti}_3\text{SiC}_2/\text{SiC}$ Composite by Hot-pressing Synthesis," postdoctoral research report, Northwestern Polytechnical University, Xi'an, China, 2001.
- [16] M.W. Barsoum, T. El-Raghy, J. Electrochem. Soc. 144 (1997) 2508.
- [17] R. Mitra, V.V. Rama, Metall. Mater. Trans., A 29 (1998) 1665.